

Combustion Pathways of the Alkylated Heteroaromatics: Bond Dissociation Enthalpies and Alkyl Group Fragmentations[†]

Carrigan J. Hayes and Christopher M. Hadad*

Department of Chemistry, The Ohio State University, 100 West 18th Avenue, Columbus, Ohio 43210

Received: October 22, 2008; Revised Manuscript Received: March 13, 2009

The bond dissociation enthalpies (BDEs) of the alkyl groups of the alkyl-substituted heterocycles have been studied and compiled using DFT methodology, with the intent of modeling the larger heterocyclic functionalities found in coal. DFT results were calibrated against CBS-QB3 calculations, and qualitative trends were reproduced between these methods. Loss of hydrogen at the benzylic position provided the most favorable route to radical formation, for both the azabenzenes and five-membered heterocycles. The ethyl derivatives had lower BDE values than the methyl derivatives due to increased stabilization of the corresponding radicals. Calculated spin densities correlated well with bond dissociation enthalpies for these compounds, while geometric effects were minimal with respect to the heterocycles themselves. Temperature effects on the bond dissociation enthalpies were minor, ranging by about 5 kcal/mol from 298 to 2000 K; the free energies of reaction dropped significantly over the same range due to entropic effects. Monocyclic heteroaromatic rings were seen to replicate the chemistry of multicyclic heteroaromatic systems.

Introduction

Coal is a valuable fossil fuel, accounting for the majority of America's electrical power generation, and it is likely to become even more useful in the years ahead, as natural gas and oil reserves dwindle.¹ The actual structure of a given coal specimen varies greatly with geography;² however, aromatic hydrocarbons and heteroaromatic rings (Figure 1), both alkylated and non-alkylated, are recurring components, the proportions of which differ between regions and samples.³

The practice of using the reactions of these individual rings to better understand the overall chemistry of the complex structure of coal has been widespread over the past few decades. In separate studies, Mackie et al. and Kiefer et al. have examined shock tube studies of pyridine, the picolines (methyl-substituted pyridines), pyrazine, and pyrimidine to better understand the thermal decompositions of coal units.⁴ These studies have focused only on pyrolysis; thus, the understanding of the oxidative decompositions of these heteroaromatics are still of interest. Moreover, Eisele established the presence of pyridine and picoline ions in the troposphere, such that the low-temperature oxidation pathways of these species are also relevant and could have implications for atmospheric processes.⁵ These heteroaromatic rings have the potential to be oxidized at the nitrogen atom and thus form NO_x species,⁶ which can subsequently react to overproduce tropospheric ozone and contribute to acid rain.⁷

Our group has devoted much time to the study of these coal constituents. Barckholtz et al. completed an exhaustive survey to select an appropriate computational method for study of these relatively large molecules; density functional theory (DFT)⁸ was shown to balance accurate results with computational economy to the greatest extent.⁹ This study also allowed the determination of a crucial conclusion, that the monocyclic heteroaromatic rings do provide constructive models for comparison to their poly-

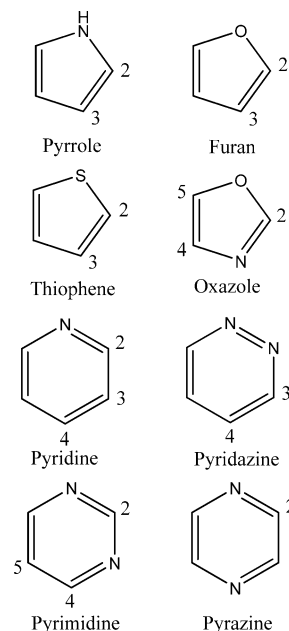


Figure 1. Aromatic heterocycles of interest in coal combustion.

cyclic analogues, via comparisons of sp² C–H bond dissociation enthalpy (BDE) values in polycyclic compounds with the corresponding BDE in the relevant monocyclic ring. The vast majority of these calculations showed that increasing the number of rings in the compound affected the BDEs by less than 1 kcal/mol, and thus, the smaller rings provide worthy, computationally prudent models for the larger systems. Moreover, it was shown that heteroatoms in the six-membered rings provided stabilization for the resulting radical, such that pyridine and other heteroaromatic rings had lower BDE values than did benzene alone.

The combustive pathways of these heteroaromatics have also been explored at multiple temperatures. Fadden et al. saw that there were considerable differences between the pathways of

[†] Part of the "Russell M. Pitzer Festschrift".

* To whom correspondence should be addressed. E-mail: hadad.1@osu.edu. Fax: 614-292-1685.

the five-membered heteroaromatics' peroxy radicals and the azabenzene's peroxy radicals;¹⁰ the former could lose atomic oxygen at a relatively low energetic cost, while for the six-membered rings, losing atomic oxygen was substantially more unfavorable, to the extent that dissociation back to the aromatic radical and molecular oxygen was preferable. For both sets of compounds, intramolecular cyclizations competed with oxygen loss, and some of these cyclizations did lead to nitroso compounds, which have implications both for NO_x formation and as carcinogens.¹¹

Computational and experimental methods clearly benefit from a symbiotic relationship in combustion studies; calculations can propose pathways for empirically observed intermediates, and experiments can verify the accuracy of the calculated energies and rate coefficients. Combustion models have been proposed for several classes of molecules, including alkyl hydrocarbons and aromatic species.

To this point, little has been published on the subject of alkylated heteroaromatic rings, though these species demonstrate comparable promise for elucidating coal chemistry. Notably, Mackie and co-workers completed both experimental^{12,13} and theoretical¹⁴ studies of the pyrolytic decomposition of 2-picoline (2-methylpyridine). However, more than a decade later, this remains the most exhaustive study of an alkylated heteroaromatic ring's combustion pathway, although the authors hypothesized that these actually provided a better model for fuel-bound nitrogen (FBN) than did unsubstituted heteroaromatic rings, which have been more common targets.^{4–10} The kinetics of the methyl-substituted azabenzene's initial reactivities have been explored more frequently; Frerichs et al. examined the reaction of the picolines with atomic oxygen,¹⁵ while Yeung and Elrod completed a study of hydroxyl radical's reactions with pyridine and its methyl- and ethyl-substituted derivatives.¹⁶ Both groups noted similarities between the alkylated azabenzene and the reactivity of toluene.

Unsurprisingly, with respect to toluene and the other alkylated aromatic hydrocarbons, more references are available. Both experimental and theoretical studies have been completed on the combustion processes of toluene. Most recently, Pitz et al. published a comprehensive mechanistic study using shock tube techniques;¹⁷ earlier studies had dealt specifically with improving predictions of some of the key intermediates therein.¹⁸ Computationally, substituent effects are a popular area of study, as well as the overall mechanism; the hydrogen-atom-loss and subsequent atmospherically relevant reactions of toluene have been studied via semiempirical methods¹⁹ and the B3LYP functional.²⁰ Nam et al. completed a DFT study of toluene and its para- and meta-substituted derivatives, observing how substituents on the methyl group itself further impact the bond dissociation enthalpies of these species.²¹ Ethylbenzene has been subjected to several studies; its pyrolysis²² and its reactions with atomic oxygen,²³ a fluorine radical,²⁴ a hydrogen atom,²⁵ a hydroperoxyl radical,²⁶ and a benzyl radical²⁷ have been studied. These hydrocarbon compounds can provide references for energies and likely pathways for the corresponding alkylated heteroaromatic rings.

Of greatest interest to this particular work are the bond dissociation enthalpies (BDEs) of toluene and ethylbenzene. Besides these species' use as reference compounds for the substituted heteroaromatics, they are also of interest as intermediates in the HACA (H abstraction–C₂H₂ addition) pathway to soot formation.²⁸ A necessary first step in any combustion pathway is generation of a radical species that can be subsequently oxidized, and this homolytic cleavage is represented

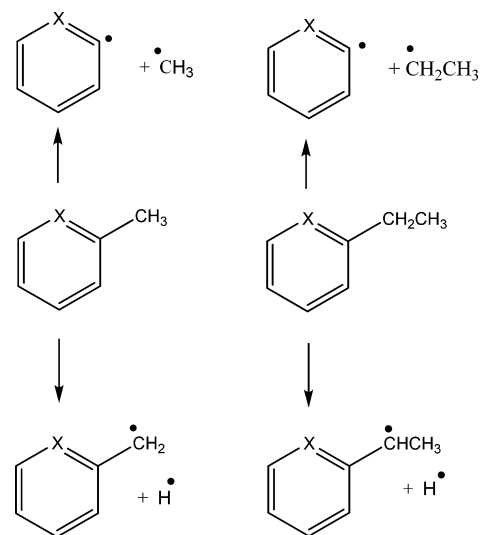


Figure 2. Generic representation of possible radical generation pathways for the alkylated heteroaromatic rings.

quantitatively via BDEs. The BDEs of toluene's methyl group and ethylbenzene's benzyl position have been experimentally determined by several methods, including flowing afterglow mass spectrometry, shock tubes, and photoacoustic calorimetry; these were recently compiled by Muralha et al.²⁹ The BDE values calculated for toluene varied from 88.0³⁰ to 90.3 kcal/mol,³¹ with the majority of results falling in the 89.5–90 kcal/mol range. With ethylbenzene, the resulting radical saw stabilization from the additional alkyl group; therefore, its BDE was lower, ranging from 85.4 to 86.9 kcal/mol.^{29,32,33}

In general, bond dissociation enthalpies are useful quantities in terms of predicting relative reactivities for different compounds, reflecting the enthalpy change for homolytic cleavage of a given bond. The more stable the resulting radical, the more likely a bond is to break. General explanations for radical stability include alkyl substitution and resonance effects; Gronert has recently suggested an alternative explanation, that the potential for release of 1,3-repulsive energy (strain) has the greatest effect on these quantities; that is, a tertiary radical is more stable than a primary radical not because of the larger number of alkyl substituents in the radical but because of the greater magnitude of the geminal interactions in the parent hydrocarbon that are relieved upon C–H bond cleavage.³⁴

The BDEs of the alkylated heteroaromatics are expected to reflect the resonance stability of the formed radicals via conjugation to the aromatic system and the stabilizing/destabilizing role of the relevant heteroatom(s). Hydrogen-atom loss seems to be the most likely initiation step in the combustion of the alkylated heteroaromatic rings, although other pathways, such as loss of the alkyl group, are also plausible (Figure 2).³⁵ These cleavage pathways will be chain-propagating for the combustion process and may dominate at higher temperatures due to the favorable entropic term.

Just as alkylated aromatic rings are widespread in petroleum compounds, alkylated heteroaromatic rings are prevalent in coal compounds, and their combustion pathways are thus noteworthy. Thus, the hydrogen-atom-loss reactions and alkyl-radical-loss reactions for the methyl- and ethyl-substituted five- and six-membered heteroaromatic rings will be explored via DFT methods, with the goal of further elucidating the chemistry of the larger heterocyclic systems found in coal. Additionally, the DFT results will be calibrated against composite-level data, with the intent of exploring the DFT methods as economical ap-

proaches with which to further explore the oxidative pathways of the consequent radicals.

Computational Methods

All geometry optimizations, vibrational frequency calculations, and single-point energy calculations were completed with Gaussian 98³⁶ and 03³⁷ at the Ohio Supercomputer Center. Several methods were initially considered for this study, as outlined in the Discussion; two hybrid density functional theory (DFT)^{38,39} approaches, B3LYP/6-31G* and BB1K/6-31+G**, were subsequently used for all geometry optimizations and vibrational frequency calculations. Single-point energies were calculated at the B3LYP/6-311+G** and BB1K/6-311+G** levels using six Cartesian d functions with the scf=tight option. CBS-QB3 calculations⁴⁰ were also performed to validate the DFT method for these particular systems. These methods comprised the bulk of the calculations; additional calibrations were also performed using MPW1K⁴¹ and G3MP2B3⁴² calculations and are noted in the text.

Vibrational frequencies were calculated for each stationary point to characterize these structures as minima or transition states. The unscaled vibrational frequencies were used to calculate the thermodynamic corrections to the enthalpy and free energy. Once obtained, zero-point vibrational energy corrections were scaled⁴³ by a factor of 0.9806 or 0.9561 for the B3LYP and BB1K calculations, respectively. The overall enthalpy at each temperature was determined from the single-point energy, the thermal correction to the enthalpy, and the scaled zero-point energy, while the overall free energy at each temperature also included the entropic correction to the free energy.

For the doublet radical species and many transition states, spin contamination ($\langle S^2 \rangle$) was negligible (no greater than 0.80). The DFT methods employed in this work have demonstrated an ability to minimize spin contamination for the radicals of interest, keeping the computed $\langle S^2 \rangle$ values near the expected value of 0.75. Spin densities were obtained for the hydrogen-loss radicals using the natural population analysis (NPA) method.⁴⁴

Because flame processes are some of the reactions of interest for these compounds, it is necessary to see how these species react at higher temperatures. The enthalpies of both the parent compounds and the resultant radicals were calculated from 298 to 2000 K via the temperature-dependent term⁴⁵

$$\Delta H(T) = H_{\text{trans}}(T) + H_{\text{rot}}(T) + H_{\text{vib}}(T) + RT$$

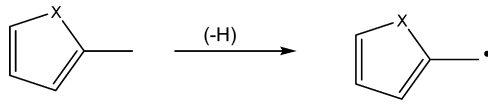
$$\Delta H(T) = \frac{3}{2}RT + \frac{3}{2}RT + Nh \sum_i v_i (e^{h\nu_i/kT} - 1)^{-1} + RT$$

The summation takes place over all $3N - 6$ normal modes. For each compound, the scaled zero-point energy and enthalpy contribution were computed at various temperatures via the given equations and added to the B3LYP total energy to obtain the bond dissociation enthalpies as a function of temperature. A similar approach was used with calculation of the entropic corrections to determine the free energies of reaction over the same temperature range.⁴⁶

Results

Several alkylated heteroaromatic rings were examined: pyrrole, furan, thiophene, oxazole, pyridine, pyrimidine, pyridazine, and pyrazine (Figure 1). Bond dissociation enthalpies (BDEs) and energies were compiled for the benzyl C–H BDE in both the methyl and ethyl derivatives of these compounds, as were

TABLE 1: Bond Dissociation Enthalpies^a (ΔH_{298} , kcal/mol) for H-Atom Loss from the Methyl Group of the 2-Methyl-Substituted Heterocycles of Interest



	CBS-QB3	G3MP2B3	B3LYP	MPW1K	BB1K
pyrrole	86.7	87.7	83.1	83.3	85.2
furan	86.3	87.9	83.1	82.9	85.2
thiophene	86.5	88.6	83.0	83.0	85.3
oxazole	89.9	91.6	86.4	86.6	88.8
pyridine	92.0	93.8	88.2	87.4	90.1
pyrimidine	93.1	94.9	89.5	88.8	91.5
pyrazine	92.3	94.5	88.0	87.1	89.8

^a Enthalpies at 298 K were taken directly from composite method calculations (CBS-QB3 and G3MP2B3). Enthalpies at 298 K were generated for the DFT calculations using single-point energies in tandem with thermal corrections to the enthalpy and scaled zero-point energies; single-point energies were calculated at the following levels: B3LYP = B3LYP/6-311+G(d,p)//B3LYP/6-31G(d); MPW1K = MPW1K/6-311+G(d,p)//MPW1K/6-31+G(d,p); BB1K = BB1K/6-311+G(d,p)//BB1K/6-31+G(d,p).

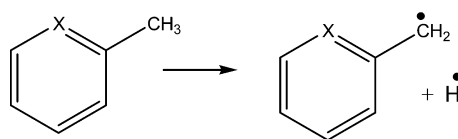
the corresponding spin densities in the derived radicals. Enthalpies and free energies of reaction for loss of the attached alkyl groups were also documented. BDE values were then analyzed as a function both of excess spin density on the major radical center of interest and of temperature. Finally, the harmonic oscillator and hindered rotor approximations were compared.

Discussion

Several trends can be observed from the enthalpic and free-energy data; for simplicity's sake, these trends will be discussed in terms of the relative bond dissociation enthalpies. Moreover, we will use the term "heteroaromatic ring" generally to refer to the five- and six-membered aromatic heterocycles under consideration. Finally, the nomenclature used will indicate that all radicals are located on the benzylic position of the compound; that is, 2-methylpyridinyl radical will be used as an abbreviation for the 2-methylpyridin-2'-yl (C-C₅H₄N-CH₂*) radical throughout the paper.

With respect to determining a useful computational approach, several methods were initially employed (Table 1) for a representative survey of relevant bond dissociation enthalpies (BDEs). The composite methods G3MP2B3 and CBS-QB3 calculated similar thermochemistry, while the DFT methods B3LYP, BB1K, and MPW1K predicted BDE values generally 2–4 kcal/mol lower than those returned by the composite methods. A more comprehensive set of calculations was completed using the CBS-QB3, B3LYP, and BB1K methods (Table 2) to more fully understand these trends. The composite methods replicated experimental results, where available. The DFT methods did not demonstrate a comparable quantitative accuracy but did replicate qualitative trends, suggesting that an empirical correction might prove useful in kinetic applications of these data. These points will be revisited throughout this discussion. We have also explored several trends and effects as functions of the B3LYP geometries, given their relevance to both the DFT and CBS-QB3 calculations.

Toluene As a Reference Compound. The BDE and geometry of toluene were both explored, along with those of the substituted heteroaromatic rings. Since more information is available for toluene, it can serve as a standard for evaluating

TABLE 2: Thermodynamic Information and Spin Density Information for Hydrogen-Loss (C–H homolytic bond cleavage) Reactions of Methyl-Substituted Heteroaromatic Rings^a

	methyl subst.	ΔH_{298}				ΔG_{298}			spin density ($\alpha-\beta$)
		B3LYP	BB1K	CBS	experimental	B3LYP	BB1K	CBS	
toluene	1	86.7	88.5	90.6	88.0–90.3 ^b	79.4	81.2	83.8	0.72
pyrrole	2	83.1	85.2	86.7		75.2	77.4	78.9	0.63
	3	86.8	88.8	90.1		78.9	80.9	82.4	0.74
furan	2	83.1	85.2	86.3		75.3	77.3	78.6	0.60
	3	87.4	89.4	90.5		79.5	81.4	82.7	0.73
thiophene	2	83.0	85.3	86.5		75.2	77.5	79.1	0.59
	3	86.9	88.9	89.9		79.1	81.0	82.2	0.71
oxazole	2	86.4	88.8	89.9		78.7	81.0	82.3	0.64
	4	88.1	90.0	91.1		80.2	82.0	83.3	0.72
	5	84.5	86.5	87.9		76.6	78.6	80.1	0.63
pyridine	2	88.2	90.1	92.0	96.0 ^c	80.8	82.5	84.7	0.73
	3	87.0	88.9	91.0		79.7	81.4	83.7	0.72
	4	87.9	89.7	91.6		80.8	82.5	84.6	0.74
pyridazine	3	88.9	90.7	93.3		81.3	83.2	85.8	0.75
	4	87.7	89.5	91.7		80.3	82.4	84.6	0.72
pyrimidine	2	89.5	91.5	93.1		82.5	84.5	86.7	0.76
	4	89.3	91.3	92.7		81.9	83.7	85.5	0.75
	5	87.5	89.3	91.4		80.6	82.1	84.7	0.73
pyrazine	2	88.0	89.8	92.3		80.5	82.2	85.0	0.72

^a Enthalpies and energies in kcal/mol, obtained via B3LYP/6-311+G**//B3LYP/6-31G* (designated as B3LYP), BB1K/6-311+G**//BB1K/6-31+G** (designated as BB1K), and CBS-QB3 (designated as CBS) methods. See Figure 1 for structures and numbering. ^b References 24–26. ^c Reference 13.

the accuracy of the computational approach, which can then be applied to the heteroaromatic rings as well.

As shown in the Supporting Information, the B3LYP/6-31G* method matched experimental values for toluene's geometry very well; both the C–C and C–H bond lengths are reproduced when compared to the spectroscopic work of Amir-Ebrahimi et al.,⁴⁷ and the rotational constants similarly match up. The vibrational frequencies, also reported in the Supporting Information, saw a comparable correspondence.

Comparable information on the benzyl radical was not readily available; however, it can be inferred from the bond dissociation enthalpy of toluene as both parent and radical must necessarily be geometrically correct to give an accurate BDE value. The CBS-QB3 calculations predict a BDE of 90.6 kcal/mol, matching well with the experimental data (a range of 88.0–90.3 kcal/mol). The B3LYP/6-311+G**//B3LYP/6-31G* energies ultimately provide a calculated BDE of 86.7 kcal/mol, while the BB1K/6-311+G**//BB1K/6-31+G** energies yielded a calculated BDE of 88.5 kcal/mol; the ~2–4 kcal/mol differences from the CBS-QB3 calculations are consistent throughout the heteroaromatic rings studied, such that qualitative trends are reproduced. The underestimate relative to composite methods is common to DFT approaches and is seen in other work in this area.⁹

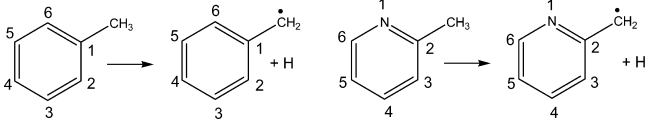
Nonalkylated Heteroaromatics. Azabenzene. Just as this work uses toluene and ethylbenzene as benchmarks for the alkylated heteroaromatic rings, previous work on the unsubstituted heteroaromatic rings has shown several trends in their BDEs relative to that of benzene.⁹ With respect to the azabenzene, it was seen that the presence of one or more nitrogen atoms within the aromatic ring directly affected those compounds' BDEs. In particular, the BDE at the C–H bond adjacent to nitrogen was consistently seen to be around 4–5 kcal/mol lower than benzene's C–H BDE, a phenomenon attributed to

nitrogen's ability to lend greater resonance stabilization to the heterocyclic radical. At the non-nitrogen-adjacent positions, the C–H BDE was comparable to that of benzene itself.

Five-Membered Heteroaromatics. Prior work on the unsubstituted five-membered heteroaromatic rings has shown that their combustion pathways are most likely to begin with decomposition or isomerization of the ring itself, rather than loss of a hydrogen atom.⁹ This is due to the geometric perturbation introduced by forming a radical centered on the aromatic ring, which is reflected in the higher C–H BDE values compared to those of benzene. Furthermore, unlike the azabenzene, there is no distinct preference of H abstraction from position 2 over position 3; again, due to geometric factors, the heteroatoms are unable to stabilize the radical to the degree seen in the six-membered rings.

Shifting focus to the alkylated heteroaromatic rings, it seems probable that the chemistry here could differ substantially since these H-loss reactions will not create a radical center within the aromatic ring itself but rather on the attached alkyl group. This proves to be the case as these trends differ from those of the unsubstituted compounds.

Methyl-Substituted Heteroaromatics: Hydrogen Atom Loss. Azabenzene. As calculated via B3LYP, the methyl-substituted azabenzene vary in their BDEs from 87.0 to 89.5 kcal/mol, with an average value of 88.2 kcal/mol, higher than toluene's value of 86.7 kcal/mol; via BB1K, this range is 88.9–91.5 kcal/mol, with an average value of 90.1 kcal/mol, compared to toluene's BDE of 88.5 kcal/mol (Table 2). The experimental work of Doughty and Mackie on 2-methylpyridine¹⁴ did provide a tangential reference point here; their proposed C–H BDE was 96 kcal/mol, compared to the calculated value of 88.2 kcal/mol via B3LYP (92.0 kcal/mol via CBS-QB3). Calculations were seen to underestimate the BDE by a slightly greater margin than that in toluene's case.

TABLE 3: Comparison of Changes in Bond Lengths (Angstroms) and Bond Angles (degrees) during the Hydrogen-Atom-Loss Reactions of Toluene and Its Nitrogen Analogue, 2-Methylpyridine, As Determined via Optimization at the B3LYP/6-31G* Level


bond lengths	parent	radical	change	bond lengths	parent	radical	change
C6–C1	1.401	1.427	0.026	N1–C2	1.345	1.372	0.027
C1–C2	1.401	1.427	0.026	C2–C3	1.401	1.425	0.024
C2–C3	1.396	1.389	–0.007	C3–C4	1.394	1.389	–0.005
C3–C4	1.396	1.403	0.007	C4–C5	1.393	1.399	0.006
C4–C5	1.396	1.403	0.007	C5–C6	1.396	1.405	0.009
C5–C6	1.396	1.389	–0.007	C6–N1	1.337	1.326	–0.011
C1–Cmeth	1.512	1.407	–0.105	C2–Cmeth	1.509	1.408	–0.101

bond angles	parent	radical	change	bond angles	parent	radical	change
C6–C1–Cmeth	121.4	121.4	0	N–C2–Cmeth	116.3	117.2	0.9
C2–C1–Cmeth	120.1	121.4	1.3	C3–C2–Cmeth	121.7	121.6	–0.1
C1–Cmeth–H	110.5	121.2	10.7	H–Cmeth–C2	111.8		
C1–Cmeth–H	110.1	121.2	11.1	H–Cmeth–C2	110.4	119.6	9.2
C1–Cmeth–H	112.3			H–Cmeth–C2	110.4	121.3	11.1

The authors noted that the heat of formation for their 2-picolinyl radical was an estimate,¹⁴ which would extend to the extrapolated BDE of interest and could explain this discrepancy. Losing hydrogen from the attached methyl group rather than from the ring itself means that the resultant radical is not directly on the ring and not as directly stabilized by nitrogen's additional resonance effects. Moreover, the trend of the ortho-substituted compound's BDE being lower than that of the other substituted compounds is not duplicated here; in fact, 2-methylpyridine, 2-methylpyrimidine, and 3-methylpyridazine all have higher BDEs than their counterparts.

Both geometries and spin densities were examined to discern the origin of these effects. The geometry changes involved are minimal, as shown (Table 3). Virtually the same changes occur for toluene losing a hydrogen atom from the methyl group as for 2-methylpyridine. Spin density (population) appears to be the most logical candidate for rationalizing these trends. From the relative electron distribution ($\alpha-\beta$) between the benzyl radical and 2-methylpyridinyl radical (Figure 3), it can be seen that 2-methylpyridinyl radical localizes its electron density on the CH₂ carbon to a greater extent than the benzyl radical; correspondingly, the benzyl radical sees more electron density delocalized through the ring and a resultant stabilization. In particular, the excess spin density is localized on the positions ortho and para to the attached methyl group, and the nitrogen of the 2-methylpyridinyl radical bears less spin density than does the corresponding carbon in the benzyl radical. Similar trends were seen for the other methyl-substituted heteroaromatics (and will be discussed subsequently), although this is the most direct comparison possible. Interestingly, the ethyl-substituted heteroaromatic rings' trends are reversed relative to ethylbenzene.

Five-Membered Rings. In another marked difference from the unsubstituted heteroaromatic rings, the five-membered, methyl-substituted heteroaromatic rings consistently demonstrate BDEs lower than any of their six-membered counterparts, including toluene. Because the radical center is removed from the ring, the geometric perturbations that affected the unsubstituted compounds are no longer a major concern. Moreover, loss of hydrogen atom from the methyl group forms an allylic radical, which can now maintain the planarity necessary for delocalization.

The 2-methyl-substituted, five-membered heteroaromatic rings have lower BDEs than their 3-methyl-substituted counterparts. Presumably, the trend seen in the unsubstituted azabenzenes helps to rationalize the results seen here; the compounds in which the methyl group is ortho to the heteroatom are more able to exploit the additional resonance stability afforded by nitrogen, oxygen, and sulfur relative to carbon.

Heteroatom identity does not have a large effect on energetics for the five-membered rings, the only set of compounds for which the heteroatom was varied. The 2-methyl-substituted monoheteroaromatic rings, in particular, have virtually identical BDEs. In the methyl derivatives of oxazole, the heteroaromatic ring containing both oxygen and nitrogen, it appears that the oxygen has a more stabilizing effect than nitrogen on the resulting radical, as the 5-methyl derivative (ortho to oxygen)

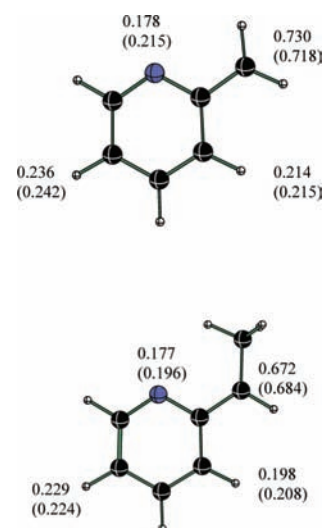


Figure 3. Comparison of areas of increased spin densities ($\alpha-\beta$) for the 2-methylpyridinyl radical and 2-ethylpyridinyl radical. The top number refers to the $\alpha-\beta$ value for that particular position; the bottom number, in parentheses, refers to the corresponding $\alpha-\beta$ value for the hydrocarbon equivalent (the benzyl radical and ethylbenzyl radical, respectively). Data obtained via B3LYP/6-311+G**//B3LYP/6-31G* calculations.

TABLE 4: Thermodynamic and Spin Density Information for Reactions of Ethyl-Substituted Heteroaromatic Rings For Hydrogen Loss from the CH₂ Group^a

	ethyl subst.	ΔH_{298}				ΔG_{298}			spin density ($\alpha-\beta$)
		B3LYP	BB1K	CBS	experimental	B3LYP	BB1K	CBS	
ethylbenzene	1	82.9	84.8	88.1	85.4–86.9 ^b	75.2	76.9	79.7	0.68
pyrrole	2	80.6	82.8	84.6		71.9	73.6	75.9	0.61
	3	84.1	85.9	87.7		75.3	77.2	78.9	0.71
furan	2	80.2	82.4	83.9		71.9	73.7	75.5	0.58
	3	84.5	86.3	87.9		75.5	77.7	79.1	0.69
thiophene	2	79.8	81.8	83.8		71.2	73.1	75.2	0.56
	3	84.4	86.1	87.1		75.4	77.1	78.1	0.67
oxazole	2	82.0	84.1	86.5		73.9	75.9	78.4	0.62
	4	84.5	86.2	88.3		76.0	77.6	79.9	0.68
pyridine	5	81.1	83.0	85.6		72.6	74.4	77.1	0.59
	2	84.2	86.2	88.1		75.0	78.1	80.0	0.69
	3	83.1	85.1	85.6		74.6	77.3	77.2	0.69
pyridazine	4	83.6	86.2	87.2		74.5	78.3	78.7	0.69
	3	85.3	86.8	90.1		76.7	79.1	83.1	0.68
pyrimidine	4	83.1	85.2	88.7		74.4	76.9	79.7	0.66
	2	84.0	86.0	89.0		76.1	77.8	80.9	0.69
pyrazine	4	84.7	87.3	88.5		76.2	79.0	80.4	0.69
	5	84.4	85.9	89.1		75.4	77.8	80.5	0.68
	2	83.9	85.8	90.2		75.6	77.7	81.4	0.66

^a Enthalpies and energies in kcal/mol, obtained via B3LYP/6-311+G**/B3LYP/6-31G* (designated as B3LYP), BB1K/6-311+G**/BB1K/6-31+G** (designated as BB1K), and CBS-QB3 (designated as CBS) methods. See Figure 1 for structures and numbering. ^b References 24, 27, and 28.

TABLE 5: Enthalpies and Free Energies of Reaction (kcal/mol) for Alkyl Group Loss Reactions of Methyl- and Ethyl-Substituted Heteroaromatics Via DFT Calculations

		B3LYP/6-311+G**/B3LYP/6-31G*						BB1K/6-311+G**/BB1K/6-31+G**					
		methyl	ΔH_{298}	ΔG_{298}	ethyl	ΔH_{298}	ΔG_{298}	methyl	ΔH_{298}	ΔG_{298}	ethyl	ΔH_{298}	ΔG_{298}
pyrrole	2	104.7	92.3	2	100.8	87.0	2	110.8	98.6	2	107.6	93.7	
	3	102.8	90.7	3	99.4	85.6	3	108.9	96.8	3	105.8	92.1	
furan	2	107.3	95.1	2	103.7	90.0	2	113.2	101.0	2	110.2	96.2	
	3	104.3	92.1	3	100.8	86.9	3	110.5	98.4	3	107.4	93.6	
thiophene	2	102.5	90.3	2	99.1	85.3	2	108.7	96.6	2	105.7	91.9	
	3	99.4	87.2	3	95.9	82.0	3	105.9	93.7	3	102.7	88.8	
oxazole	2	108.4	96.3	2	104.9	91.1	2	114.6	102.5	2	111.3	97.5	
	4	105.5	93.3	4	102.2	88.2	4	111.8	99.6	4	108.8	94.8	
pyridine	5	109.3	97.1	5	106.0	92.1	5	115.7	103.4	5	112.5	98.6	
	2	92.7	81.0	2	88.6	74.7	2	99.1	87.2	2	95.8	82.0	
	3	96.8	85.1	3	92.3	78.5	3	103.6	91.9	3	99.9	86.3	
pyridazine	4	96.2	84.8	4	91.9	78.1	4	102.6	91.1	4	99.2	85.5	
	3	94.7	82.7	3	91.4	77.8	3	101.5	89.7	3	98.5	85.4	
pyrimidine	4	95.6	84.1	4	91.7	77.9	4	103.2	91.9	4	100.1	86.4	
	2	95.9	84.6	2	92.3	78.8	2	102.2	90.9	2	99.4	85.7	
pyrazine	4	93.1	81.4	4	89.2	75.6	4	99.8	87.9	4	97.1	83.3	
	5	98.2	87.0	5	94.9	81.1	5	105.3	93.9	5	102.3	88.7	
	2	93.4	81.6	2	89.2	75.9	2	100.3	88.4	2	96.9	83.1	

alone) has a lower BDE than the 4-methyl derivative (ortho to nitrogen alone).

Ethyl-Substituted Heteroaromatics: Hydrogen Atom Loss. Overall, the ethyl-substituted heteroaromatic rings have considerably lower BDEs than their methyl counterparts; the additional alkyl group serves to stabilize the radical derived from hydrogen atom loss, regardless of ring size, by 2 to 5 kcal/mol (Table 4).

Azabenzene. The BDE values for the ethyl-substituted azabenzene actually encompass the value calculated for ethylbenzene. The narrower range and lack of any trend relative to ethylbenzene suggest that the additional methyl group present stabilizes all of the relevant radicals to a comparable extent.

Five-Membered Rings. The same trend seen with the methyl-substituted heteroaromatics is repeated here: the 2-substituted compounds have substantially lower BDEs, again due to their increased proximity to the stabilizing heteroatom. Moreover,

these compounds demonstrate more of a heteroatom effect, although it is a slight trend; the larger the heteroatom, the lower the BDE. Presumably, polarizability effects in stabilizing the radical might become more visible as the number of electrons in the molecule increases.

Methyl-Substituted Heteroaromatic Rings: Methyl Loss. Scission of the C_{ring}–C_{alkyl} bond for all of these compounds leads to an in-plane sp² aromatic radical, localized in the σ system of the aromatic ring. It was expected that the thermodynamics of these reactions would compare well to those for H-atom loss from the unsubstituted heteroaromatic rings, and this was confirmed to be the case (Table 5). Moreover, the thermochemistry for the loss of these alkyl groups was considerably more endothermic and endoergic, in all cases, than hydrogen-atom loss.

Azabenzene. Loss of the methyl group was seen to be around 10 kcal/mol more endothermic than loss of hydrogen, for any

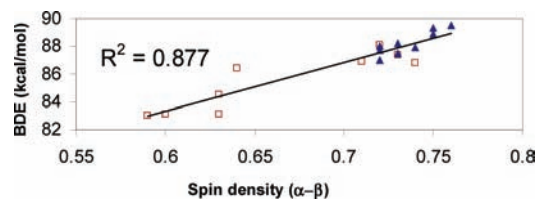


Figure 4. Variation of bond dissociation enthalpy (kcal/mol) with excess spin density at the incipient CH_2 radical center for methyl-substituted heteroaromatic rings. Data for the five-membered heteroaromatic rings are denoted by open squares; data for the six-membered heteroaromatic rings are denoted by closed triangles. Data obtained via B3LYP/6-311+G**//B3LYP/6-31G* calculations.

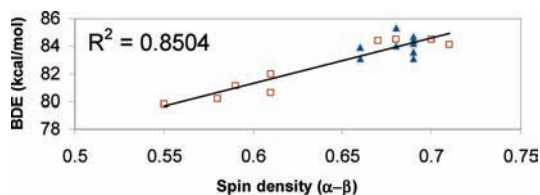


Figure 5. Variation of bond dissociation enthalpy (kcal/mol) with excess spin density at the incipient C–H radical center for ethyl-substituted heteroaromatics. Data for the five-membered heteroaromatic rings are denoted by open squares; data for the six-membered heteroaromatic rings are denoted by closed triangles. Data obtained via B3LYP/6-311+G**//B3LYP/6-31G* calculations.

given position in these compounds. Moreover, when the methyl group in question was ortho to nitrogen (as with 2-methylpyridine compared to the other pyridine derivatives and 3-methylpyridazine compared to 4-methylpyridazine), the corresponding C–C BDE was lower due to the stabilizing effects of the adjacent nitrogen.⁹ With the pyrimidine derivatives, the trend is still evident; 4-methylpyrimidine, with its methyl group between two nitrogens, has a substantially lower BDE than any other in this group.

Five-Membered Rings. The trends seen for hydrogen-loss reactions are nonexistent here. As seen in earlier work by our group⁹ and others,⁴⁸ any stabilizing effects of the nearby heteroatom are negated by the geometric strain introduced by forming a ring-centered radical; the BDE at the 2-position is generally 2 to 3 kcal/mol higher than that at the 3-position. No definite heteroatom trends are evident, and the oxazole derivatives demonstrate that the presence of two heteroatoms does not lead to greater reactivity at any one position.

Ethyl-Substituted Heteroaromatic Rings: Ethyl Loss. The ethyl-substituted compounds (Table 5) have the same trends as the methyl derivatives and therefore will not be discussed further, save to note that the BDE values are again around 5 kcal/mol lower than those of the methyl compounds, probably due to the increased stability of the primary ethyl radical over the methyl radical.

General Trends. Spin Density. The spin densities were calculated via Natural Population Analyses⁴⁴ at the B3LYP/6-311+G**//B3LYP/6-31G* level for the methyl-substituted heteroaromatic rings. Excess spin density ($\alpha-\beta$) was determined for each of the incipient CH_2 radical centers, and the BDE was plotted as a function of this quantity (Figure 4). A comparable graph of the BDE as a function of excess spin density was completed for the ethyl-substituted compounds (Figure 5). The spin density generated at the incipient radical correlated well with the BDE regardless of ring size or substitution, suggesting that the more localized a resulting radical will be, the higher the BDE value (or the more that electron delocalization will stabilize a given radical, the lower that the BDE for its corresponding parent compound will be). The correlation

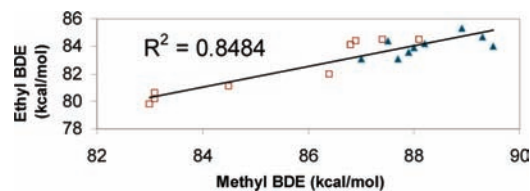


Figure 6. Correlation between bond dissociation enthalpies for methyl- and ethyl-substituted derivatives of the five-membered heteroaromatics. Data for the five-membered heteroaromatic rings are denoted by open squares; data for the six-membered heteroaromatic rings are denoted by closed triangles. Data obtained via B3LYP/6-311+G**//B3LYP/6-31G* calculations.

TABLE 6: Changes in Bond Lengths (Angstroms) and Bond Angles (degrees) for the Hydrogen-Loss Reaction of Representative Heteroaromatic Ring 2-Methylfuran As Obtained via Optimization at the B3LYP/6-31G* Level

	compound	radical	change in bond length
O–C2	1.371	1.390	0.019
C2–Cmeth	1.479	1.377	–0.102
C2–C3	1.364	1.411	0.047
C3–C4	1.436	1.411	0.025
C4–C5	1.359	1.373	–0.14
C5–O	1.366	1.361	–0.005
Cmeth–H	1.097	1.083	–0.14

	compound	radical	change in bond angle
O–C2–Cmeth	116.64	118.93	2.29
C3–C2–Cmeth	133.82	133.17	–0.65
H1–Cmeth–C2	111.57		
H2–Cmeth–C2	111.57	120.93	9.36
H3–Cmeth–C2	109.87	120.06	10.19
H1–Cmeth–H2	108.17		
H2–Cmeth–H3	107.36	119.01	11.65
H3–Cmeth–H1	108.16		

between the methyl and ethyl derivatives' respective bond dissociation enthalpies (Figure 6) was also strong ($R^2 = 0.84$).

Geometry. Several geometric changes occurred within these compounds, which can be understood by examining a repre-

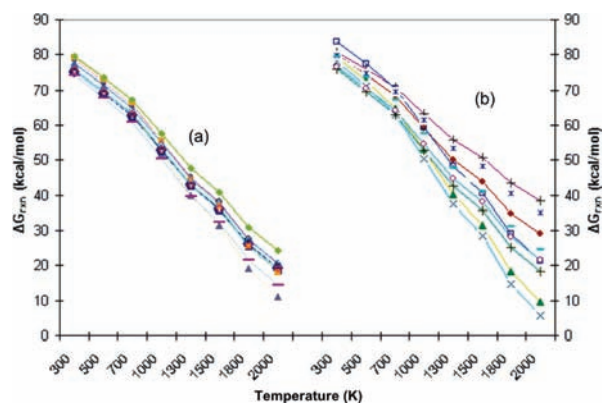


Figure 7. Variation of the free energy of reaction (kcal/mol) with temperature (K) for hydrogen atom loss in the (a) five-membered methyl-substituted heteroaromatic rings and (b) six-membered methyl-substituted heteroaromatic rings. Data obtained via B3LYP/6-311+G**//B3LYP/6-31G* calculations. Similar temperature profiles for the ethyl-substituted derivatives are available in the Supporting Information.

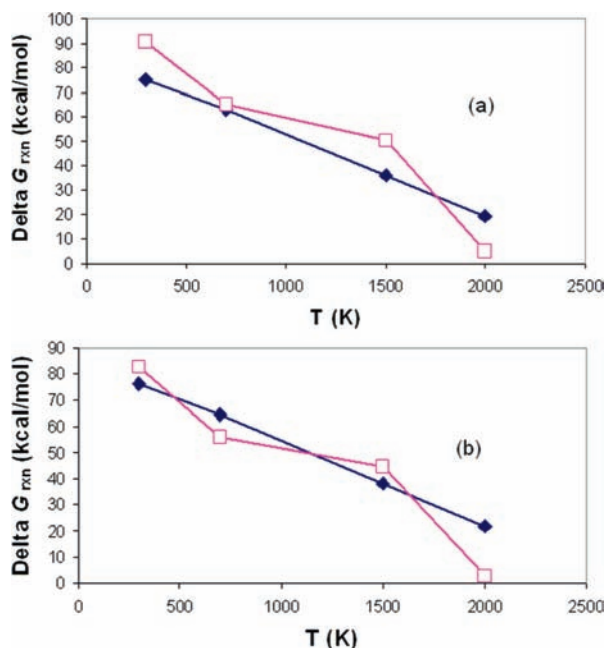


Figure 8. Comparison of hydrogen atom loss and methyl group loss free energies (ΔG_{rxn}) with increasing temperature (K). Representative pathways are shown for (a) 2-methylpyrrole and (b) 3-methylpyridazine. Free energies for hydrogen atom loss are denoted with solid diamonds and a blue line; free energies for methyl loss are denoted with open squares and a pink line. Data obtained via B3LYP/6-31+G**//B3LYP/6-31G* calculations. Graphs comparing H atom loss to ethyl group loss are available in the Supporting Information.

sentative reaction (Table 6) with 2-methylfuran. In terms of bond lengths, the main change occurred in the bond between the furan ring and alkyl chain, which shorted substantially as the bond took on more π character in the corresponding radical. Bonds within the ring lengthened to some extent. With respect to bond angles, the $\text{O}-\text{C}_2-\text{C}_{\text{meth}}$ angle increased slightly and the $\text{H}-\text{C}_{\text{meth}}-\text{C}_2$ angles increased substantially as hybridization at the radical center changed from sp^3 to sp^2 . The analogous geometries of interest for the other heteroaromatics are summarized in the Supporting Information. What is most significant is that, for these alkylated aromatics, the ring itself was relatively unperturbed, relative to previous studies in which the new radical was located directly on the heteroaromatic ring of interest.⁹

Temperature Effects. Calculations were completed to examine the changes in hydrogen-loss BDE at combustion temperatures for these compounds. Minor quantitative changes (increases of ~ 4 kcal/mol) in the hydrogen-loss BDEs of the

heterocyclic compounds occur over this temperature range; the most dramatic variation, seen with 2-methylpyrrole and 3-methylpyrrole, is still less than 10 kcal/mol. (Full profiles are available in the Supporting Information.) Thus, the 298 K enthalpic data can also be useful in terms of predicting higher-temperature chemistry. The free energies of reaction for hydrogen atom loss were also explored as a function of temperature (Figure 7); these quantities experienced a large temperature effect due to the entropic term for these dissociative processes. At high temperatures (2000 K), the free energies of reaction are roughly 60 kcal/mol more favorable than at 298 K, making these radicals ready participants in high-temperature combustion processes.

Moreover, comparative temperature profiles were generated to explore the relative energetics of hydrogen atom loss and alkyl group loss (Figure 8). Representative cases are shown; a more complete set of information is included in the Supporting Information. Both pathways see large entropic contributions at higher temperatures. In all cases, hydrogen atom loss is initially the favored pathway, but at 2000 K, alkyl group loss is favored slightly. At no temperature is one pathway overwhelmingly dominant over the other, and the energetics overlap at several points, so that the further combustion pathways of both sets of radicals will likely contribute in comparable capacity.

Approximations. Calculations were run to determine what, if any, error was introduced via using the harmonic oscillator approximation in finding the enthalpic and entropic thermal corrections.⁴⁹ As described previously, the lowest-energy vibrations (i.e., the motions of the alkyl chain) were identified and treated as rotations using a hindered rotor approximation rather than the harmonic oscillator. Briefly, the enthalpies are essentially consistent between approximations, while the free energies reflect a small change, generally less than 1 kcal/mol. Considering that this variation in approximation would have the most impact on the entropy of these species, it seems logical that the free energies would see more of an effect than the enthalpies. These specific data are included in the Supporting Information.

Extension to Larger Systems. The validity of using monocyclic systems to approximate the chemistry of multicyclic systems was explored. Previous work in our group has demonstrated that increasing the number of rings attached to a parent heteroaromatic ring has only a minor effect on the bond dissociation enthalpy for H atom loss in that parent compound,⁹ however, calculations were pursued to see if a similar effect occurred in the alkylated derivatives of these heteroaromatic rings. The H-atom-loss reactions from the methylated derivatives

TABLE 7: Comparison of ΔH_{rxn} and ΔG_{rxn} (kcal/mol) Values for H-Atom-Loss Reactions in Monocyclic and Multicyclic Heteroaromatic Systems (data calculated via B3LYP/6-311+G//B3LYP/6-31G*)**

methyl subst.	benzofuran				benzothiophene				quinoline			
	BDE	ΔBDE^a	ΔG_{rxn}	$\Delta\Delta G_{\text{rxn}}$	BDE	ΔBDE	ΔG_{rxn}	$\Delta\Delta G_{\text{rxn}}$	BDE	ΔBDE	ΔG_{rxn}	$\Delta\Delta G_{\text{rxn}}$
2	83.0	-0.1	75.1	-0.2	83.2	+0.2	75.3	+0.1	87.8	-0.5	80.1	-0.7
3	86.6	-0.8	78.5	-1.0	86.1	-0.8	78.0	-1.1	86.1	-0.9	78.4	-1.3
4									86.7	-1.2	78.5	-2.3

^a Indicates the difference between the given BDE and the corresponding BDE in the monocyclic heteroaromatic (i.e., 2-methylbenzofuran compared to 2-methylfuran).

of benzofuran, benzothiophene, and quinoline (Table 7) were explored. It was seen that generally, the BDEs in the relevant monocycles were within 1 kcal/mol of the BDEs in the multicyclic systems, reinforcing our previous findings.

Conclusions

Bond dissociation enthalpies for hydrogen loss and alkyl group loss were compiled for the alkylated heteroaromatics using a variety of DFT and composite methods. Both B3LYP and B3LYP/6-31G(d) demonstrated promise for replicating qualitative trends predicted by CBS-QB3 and G3MP2B3, although a systematic deviation of 2–4 kcal/mol was shown regardless of ring size and substitution patterns. Composite methods replicated the experimental BDEs available in the literature.

Overall, loss of hydrogen to form a benzylic-like radical was roughly 10 kcal/mol more favorable than loss of an alkyl group, regardless of ring size or heteroatom. BDE trends varied considerably with respect to ring size and bond type. For the hydrogen-loss reactions, the methyl-substituted azabenzenes saw higher BDEs than their hydrocarbon counterpart, toluene. However, the methyl-substituted five-membered heteroaromatic rings displayed consistently lower BDEs than the azabenzenes and, moreover, exhibited a trend where the 2-substituted compounds had lower BDEs than the 3-substituted compounds due to increased stabilization of the radical via increased proximity to the heteroatom. In the hydrogen-atom fragmentation reactions of the ethyl derivatives, the trends within each class of compounds (azabenzenes versus heteroaromatic rings) were duplicated, but an overall stabilization of the radicals of interest caused the BDEs of these reactions to drop by ~4 kcal/mol. In terms of alkyl group loss, the ortho-substituted azabenzenes were more able to stabilize the in-plane sp^2 radicals in these reactions due to the adjacent nitrogen atom and had consistently lower BDEs than their counterparts. The five-membered heteroaromatic rings could not exploit a similar relationship as their alkyl-loss reactions caused geometric perturbations to the ring, decreasing any aromatic contribution to resonance stability and thus increasing the BDEs for these compounds.

Spin densities were calculated for these heterocyclic radicals and correlated well with the BDE values; this was seen especially in the case of the five-membered heteroaromatics. Temperature effects were explored for the hydrogen-loss reactions and demonstrated that the reactions stayed constant in their endothermicity but became substantially less endoergic over the 298–2000 K range due to entropic effects on the free energy. The free-energy profiles of hydrogen-atom loss compared to those of alkyl group loss showed that both pathways experienced similar temperature effects. Vibrational frequencies attributed to methyl and ethyl rotations were also explored for their effect on the thermodynamic predictions using the hindered rotor approximation; this treatment gave comparable results for the enthalpies and free energies of these reactions.

With respect to predicting the chemistry of the larger heterocyclic systems found in coal, our work suggests that both hydrogen-atom-loss and alkyl-group-loss reactions will contribute as initiation steps for the high-temperature combustion reactions of these rings. Longer alkyl chains and larger ring sizes will increase reactivity. The initial steps of radical formation become much more favorable at high temperatures. The B3LYP and B3LYP/6-31G(d) methods have shown promise in economically elucidating these pathways, which has implications for exploring combustion pathways of coal compounds; the B3LYP/6-31G(d) method shows an increased quantitative accuracy relative

to other DFT methods, while the B3LYP data facilitate comparison to several previous studies of related species.^{9,10} However, their lack of quantitative comparability to the composite methods implies that an empirical correction factor would be necessary before these data could be realistically employed in any kinetic applications; the composite calculations obtain far more accurate results. Thus, while the chemistry of monocyclic heteroaromatic systems approximates that of larger heteroaromatic systems to a useful degree, economic computational exploration of the chemistry of these smaller systems still presents a challenge. These initial calculations will be revisited in further work concerning the combustion pathways of the alkylated heteroaromatics.

Acknowledgment. We dedicate this paper to Professor Russell Pitzer, an excellent and supportive colleague, who is a pioneer in electronic structure theory and a visionary for the role of computational chemistry in both theoretical and applied areas of science. This work was supported financially by the National Science Foundation (CHE-0089147), and the Ohio Supercomputer Center provided access to generous allocations of computational resources.

Supporting Information Available: Geometries, vibrational frequencies, and energetic information are included for all species, as are temperature profiles for hydrogen atom loss and alkyl group loss for all species over the temperature range of 298–2000 K, and a comparison of results obtained with the harmonic oscillator and hindered rotor approximations. This material is available free of charge via the Internet at <http://pubs.acs.org>.

References and Notes

- (1) Coal Fired Power Generation. <http://www.rst2.edu/ties/acidrain/IEcoal/how.htm> (accessed May 31, 2006).
- (2) Smith, K. L.; Smoot, L. D.; Fletcher, T. H.; Pugmire, R. J. *The Structure and Reaction Processes of Coal*; Plenum Press: New York, 1994.
- (3) (a) Axworthy, A. *Fuel* **1987**, *57*, 29–35. (b) Meyers, R. A. *Coal Structure*; Academic Press: New York, 1982.
- (4) (a) Mackie, J.; Colket, M.; Nelson, P. *J. Phys. Chem.* **1990**, *94*, 4099–4106. (b) Doughty, A.; Mackie, J. *J. Phys. Chem.* **1992**, *96*, 10339–10348. (c) Kiefer, J.; Zhang, Q.; Kern, R.; Yao, J.; Jursic, B. *J. Phys. Chem. B* **1997**, *101*, 7061–7073.
- (5) Eisele, F. L. *Int. J. Mass Spectrom. Ion Phys.* **1983**, *54*, 119–126.
- (6) Williams, A.; Pourkashanian, M.; Jones, J. M.; Rowlands, L. *J. Inst. Energy* **1997**, *70*, 102–113.
- (7) Streit, G. E.; Spall, D. E.; Hall, J. H. *Environ. Sci. Technol.* **1987**, *21*, 519–525.
- (8) (a) Parr, R. G.; Yang, W. *Density Functional Theory in Atoms and Molecules*; Oxford University Press: New York, 1989. (b) Labanowski, J. W.; Andzelm, J. *Density Functional Methods in Chemistry*; Springer: New York, 1991.
- (9) Barkholtz, C.; Barkholtz, T. A.; Hadad, C. M. *J. Am. Chem. Soc.* **1999**, *121*, 491–500.
- (10) (a) Fadden, M. J.; Hadad, C. M. *J. Phys. Chem. A* **2000**, *104*, 6088–6094. (b) Fadden, M. J.; Hadad, C. M. *J. Phys. Chem. A* **2000**, *104*, 6324–6331.
- (11) Mirvish, S. S. *Cancer Lett.* **1995**, *93*, 17–48.
- (12) Terentis, A.; Doughty, A.; Mackie, J. *J. Phys. Chem.* **1992**, *96*, 10334–10339.
- (13) Ikeda, E.; Mackie, J. *J. Anal. Appl. Pyrolysis* **1995**, *34*, 47–63.
- (14) Doughty, A.; Mackie, J. *J. Phys. Chem.* **1992**, *96*, 10339–10348.
- (15) Frerichs, H.; Schliephake, V.; Tappe, M.; Wagner, H. *Z. Phys. Chem.* **1990**, *166*.
- (16) Yeung, L.; Elrod, M. *J. Phys. Chem. A* **2003**, *107*, 4470–4477.
- (17) Pitz, W. J.; Seiser, R.; Bozzelli, J. W.; Da Costa, I.; Fournet, R.; Billaud, F.; Battin-Leclerc, F.; Seshadri, K.; Westbrook, C. K. 30th International Symposium on Combustion, July 2004.
- (18) (a) Klotz, S. D.; Brezinsky, K.; Glassman, I. *Proc. Combust. Inst.* **1998**, *27*, 337–344. (b) Emdee, J. L.; Brezinsky, K.; Glassman, I. *J. Phys. Chem.* **1992**, *96*, 2151–2161. (c) Zhong, X.; Bozzelli, J. *Int. J. Chem. Kinet.* **1997**, *29*, 893–913. (d) Zhong, X.; Bozzelli, J. *J. Phys. Chem. A* **1998**, *102*, 3537–3555. (e) Linstedt, R. P. *Combust. Sci. Technol.* **1996**, *120*, 119–

167. (f) Venkat, C.; Brezinsky, K.; Glassman, I. *Proc. Combust. Inst.* **1982**, *19*, 143–152. (g) Brezinsky, K.; Litzinger, T.; Glassman, I. *Int. J. Chem. Kinet.* **1984**, *16*, 1053–1061. (h) Griffiths, J.; Halford-Maw, P.; Rose, D. *Combust. Flame* **1993**, *95*, 291–306. (i) Roubaud, A.; Minetti, R.; Sochet, L. *Combust. Flame* **2000**, *121*, 535–541.
- (19) Wen, Z.; Li, Z.; Shang, Z.; Cheng, J.-P. *J. Org. Chem.* **2001**, *66*, 1466.
- (20) Bean, G. P. *Tetrahedron* **2002**, *58*, 9941.
- (21) Nam, P. C.; Nguyen, M. T.; Chandra, A. *J. Phys. Chem. A* **2005**, *109*, 10342–10347.
- (22) Clark, W. D.; Price, S. J. *Can. J. Chem.* **1970**, *48*, 1059–1064.
- (23) Grovenstein, E., Jr.; Mosher, A. J. *J. Am. Chem. Soc.* **1970**, *92*, 3810–3812.
- (24) Ebrecht, J.; Hack, W.; Wagner, H. *Ber. Bunsen-Ges. Phys. Chem.* **1989**, *93*, 619–623.
- (25) Ebert, K. H.; Ederer, H. J.; Schmidt, P. S.; Baulch, D. L.; Cobos, C. J.; Cox, R. A.; Esser, C.; Frank, P.; Just, T.; Kerr, J. A.; Pilling, M. J.; Troe, J.; Walker, R. W.; Warnatz, J. *J. Phys. Chem. Ref. Data* **1992**, *21*, 411–429.
- (26) (a) Baulch, D. L.; Cobos, C. J.; Cox, R. A.; Frank, P.; Hayman, G.; Just, T.; Kerr, J. A.; Murrells, T.; Pilling, M. J.; Troe, J.; Walker, R. W.; Warnatz, J. *J. Phys. Chem. Ref. Data* **1994**, *23*, 847–1033. (b) Scott, M.; Walker, R. W. *Combust. Flame* **2002**, *129*, 365–377.
- (27) Muller-Markgraf, W.; Troe, J. *J. Phys. Chem.* **1988**, *92*, 4899–4905.
- (28) (a) Frenklach, M.; Wang, H. *Proc. Combust. Inst.* **1991**, *23*, 1559–1556. (b) Wang, H.; Frenklach, M. *J. Phys. Chem.* **1994**, *98*, 11465–11489. (c) Frenklach, M. *Phys. Chem. Chem. Phys.* **2002**, *4*, 2028–2037.
- (29) (a) Hippler, H.; Troe, J. *J. Phys. Chem.* **1990**, *94*, 3803–3806. (b) Walker, J.; Tsang, W. *J. Phys. Chem.* **1990**, *94*, 3324–3327. (c) Ellison, G. B.; Davico, G. E.; Bierbaum, V. M.; DePuy, C. H. *Int. J. Mass Spectrom. Ion Proc.* **1996**, *156*, 109–131. (d) Muralha, V.; dos Santos, R.; Simoes, J. *J. Phys. Chem. A* **2004**, *108*, 936–942.
- (30) McMillen, D. F.; Golden, D. M. *Annu. Rev. Phys. Chem.* **1982**, *33*, 493–532.
- (31) Song, S.; Golden, D. M.; Hanson, R. K.; Bowman, C. T. *J. Phys. Chem. A* **2002**, *106*, 6094.
- (32) Meot-Ner, M. M.; Lias, S. G. Binding Energies Between Ions and Molecules, and the Thermochemistry of Cluster Ions. In *NIST Chemistry WebBook, NIST Standard Reference Database Number 69*; Linstrom, P. J., Mallard, W. G., Eds.; National Institute of Standards and Technology: Gaithersburg, MD, March 2003.
- (33) Smith, L., Jr.; Evans, S. J. *Chem. Soc., Perkin Trans. 2* **2000**, *7*, 1541–1551.
- (34) Gronert, S. *J. Org. Chem.* **2006**, *71*, 1209–1219.
- (35) Wallington, T. J.; Kaiser, E. W.; Farrell, J. T. *Chem. Soc. Rev.* **2006**, *35*, 335–347.
- (36) Frisch, M. J.; Trucks, G. W.; Schlegel, H. B.; Scusera, G. E.; Robb, M. A.; Cheeseman, J. R.; Zakrzewski, V. G.; Montgomery, J. A.; Stratmann, R. E., Jr.; Burant, J. C.; Dapprich, S.; Millam, J. M.; Daniels, A. D.; Kudin, K. N.; Strain, M. C.; Farkas, O.; Tomasi, J.; Barone, V.; Cossi, M.; Cammi, R.; Mennucci, B.; Pomelli, C.; Adamo, C.; Clifford, S.; Ochterski, J.; Petersson, G. A.; Ayala, P. Y.; Cui, Q.; Morokuma, K.; Malick, D. K.; Rabuck, A. D.; Raghavachari, K.; Foresman, J. B.; Cioslowski, J.; Ortiz, J. V.; Baboul, A. G.; Stefanov, B. B.; Liu, G.; Liashenko, A.; Piskorz, P.; Komaromi, I.; Gomperts, R.; Martin, R. L.; Fox, D. J.; Keith, T.; Al-Laham, M. A.; Peng, C. Y.; Nanayakkara, A.; Gonzalez, C.; Challacombe, M.; Gill, P. M. W.; Johnson, B.; Chen, W.; Wong, M. W.; Andres, J. L.; Gonzalez, C.; Head-Gordon, M.; Replogle, E. S.; Pople, J. A. *Gaussian 98*, revision A.11.03; Gaussian, Inc.: Pittsburgh, PA, 2001.
- (37) Frisch, M. J.; Trucks, G. W.; Schlegel, H. B.; Scuseria, G. E.; Robb, M. A.; Cheeseman, J. R.; Montgomery, J. A., Jr.; Vreven, T.; Kudin, K. N.; Burant, J. C.; Millam, J. M.; Iyengar, S. S.; Tomasi, J.; Barone, V.; Mennucci, B.; Cossi, M.; Scalmani, G.; Rega, N.; Petersson, G. A.; Nakatsuji, H.; Hada, M.; Ehara, M.; Toyota, K.; Fukuda, R.; Hasegawa, J.; Ishida, M.; Nakajima, T.; Honda, Y.; Kitao, O.; Nakai, H.; Klene, M.; Li, X.; Knox, J. E.; Hratchian, H. P.; Cross, J. B.; Bakken, V.; Adamo, C.; Jaramillo, J.; Gomperts, R.; Stratmann, R. E.; Yazyev, O.; Austin, A. J.; Cammi, R.; Pomelli, C.; Ochterski, J. W.; Ayala, P. Y.; Morokuma, K.; Voth, G. A.; Salvador, P.; Dannenberg, J. J.; Zakrzewski, V. G.; Dapprich, S.; Daniels, A. D.; Strain, M. C.; Farkas, O.; Malick, D. K.; Rabuck, A. D.; Raghavachari, K.; Foresman, J. B.; Ortiz, J. V.; Cui, Q.; Baboul, A. G.; Clifford, S.; Cioslowski, J.; Stefanov, B. B.; Liu, G.; Liashenko, A.; Piskorz, P.; Komaromi, I.; Martin, R. L.; Fox, D. J.; Keith, T.; Al-Laham, M. A.; Peng, C. Y.; Nanayakkara, A.; Challacombe, M.; Gill, P. M. W.; Johnson, B.; Chen, W.; Wong, M. W.; Gonzalez, C.; Pople, J. A. *Gaussian 03*, revision C.02; Gaussian, Inc.: Wallingford, CT, 2004.
- (38) (a) Becke, A. D. *Phys. Rev. A* **1988**, *38*, 3098–3100. (b) Lee, C.; Yang, W.; Parr, R. G. *Phys. Rev. B* **1988**, *37*, 785–789. (c) Becke, A. D. *J. Chem. Phys.* **1993**, *98*, 1372–1377.
- (39) Zhao, Y.; Lynch, B. J.; Truhlar, D. G. *J. Phys. Chem. A* **2004**, *108*, 2715–2719.
- (40) (a) Ochterski, J. W.; Petersson, G. A.; Montgomery, J. A., Jr. *J. Chem. Phys.* **1996**, *104*, 2598–2619. (b) Petersson, G. A.; Frisch, M. J. *J. Phys. Chem. A* **2000**, *104*, 2183–2190.
- (41) (a) Lynch, B. J.; Fast, P. L.; Harris, M.; Truhlar, D. G. *J. Phys. Chem. A* **2000**, *104*, 4811–4815. (b) Lynch, B. J.; Truhlar, D. G. *J. Phys. Chem. A* **2001**, *105*, 2936–2941.
- (42) (a) Curtiss, L. A.; Raghavachari, K.; Redfern, P. C.; Rassolov, V.; Pople, J. A. *J. Chem. Phys.* **2000**, *112*, 7374–7383. (b) Curtiss, L. A.; Redfern, R. C.; Raghavachari, K.; Pople, J. A. *J. Chem. Phys.* **2001**, *114*, 108–117.
- (43) Scott, A. P.; Radom, L. *J. Phys. Chem.* **1996**, *100*, 16502–16513.
- (44) Reed, A. E.; Weinstock, R. B.; Weinhold, F. *J. Chem. Phys.* **1985**, *83*, 735–746.
- (45) Hehre, W. J.; Radom, L.; Schleyer, P. v. R.; Pople, J. A. *Ab Initio Molecular Orbital Theory*; John Wiley and Sons: New York, 1986.
- (46) Carter, A. *Classical and Statistical Thermodynamics*; Prentice Hall: Upper Saddle River, NJ, 2001.
- (47) Amir-Ebrahimi, V.; Choplin, A.; Demaison, J.; Roussy, G. *J. Mol. Spectrosc.* **1981**, *89*, 42–52.
- (48) Bera, P. P.; Schaefer, H. F., III. *Proc. Natl. Acad. Sci. U.S.A.* **2005**, *102*, 6698–6703.
- (49) Using software designed by Dr. Timothy Barckholtz (Exxon–Mobil) obtained via private communication.

JP809356Y